OXFORD

Cerebral Cortex, 2023, **33**, 7857–7869
https://doi.org/10.1093/cercor/bhad084
Advance access publication date 18 March 2023
Original Article

Stress degrades working memory-related frontostriatal circuit function

Craig W. Berridge[1,*], David M. Devilbiss[2,†], Andrea J. Martin[1], Robert C. Spencer[1], Rick L. Jenison[1]

[1]Department of Psychology, University of Wisconsin, Madison, WI 53706, United States,
[2]Department of Cell Biology and Neuroscience, Rowan University

*Corresponding author: Department of Psychology, University of Wisconsin, 1202 West Johnson Street, Madison, WI 53706, United States. Email: berridge@wisc.edu
†2 Medical Center Drive, SC220, Stratford, NJ 08084, United States

Goal-directed behavior is dependent on neuronal activity in the prefrontal cortex (PFC) and extended frontostriatal circuitry. Stress and stress-related disorders are associated with impaired frontostriatal-dependent cognition. Our understanding of the neural mechanisms that underlie stress-related cognitive impairment is limited, with the majority of prior research focused on the PFC. To date, the actions of stress across cognition-related frontostriatal circuitry are unknown. To address this gap, the current studies examined the effects of acute noise-stress on the spiking activity of neurons and local field potential oscillatory activity within the dorsomedial PFC (dmPFC) and dorsomedial striatum (dmSTR) in rats engaged in a test of spatial working memory. Stress robustly suppressed responses of both dmPFC and dmSTR neurons strongly tuned to key task events (delay, reward). Additionally, stress strongly suppressed delay-related, but not reward-related, theta and alpha spectral power within, and synchrony between, the dmPFC and dmSTR. These observations provide the first demonstration that stress disrupts the neural coding and functional connectivity of key task events, particularly delay, within cognition-supporting dorsomedial frontostriatal circuitry. These results suggest that stress-related degradation of neural coding within both the PFC and striatum likely contributes to the cognition-impairing effects of stress.

Key words: prefrontal cortex; striatum; synchrony; delay; working memory.

The prefrontal cortex (PFC) plays a central role in regulating cognitive processes that guide flexible goal-directed behavior, including working memory (Goldman-Rakic 1996; Miller and Cohen 2001). PFC-dependent cognition involves topographically organized connections with the striatum (Heilbronner et al. 2016). For example, in rodents, the dorsal aspect of the medial PFC is closely associated with higher cognitive function and extends a robust innervation to the dorsomedial striatum (dmSTR; Voorn et al. 2004). Importantly, lesion and inactivation studies demonstrate that multiple PFC-dependent cognitive processes, including working memory, are similarly dependent on the dmSTR (Goldman and Rosvold 1972; Ragozzino 2007; Spencer et al. 2012; Spencer and Berridge 2019). Collectively, these findings identify a central role of frontostriatal circuitry in higher cognitive function.

It has long-been known that stress impairs cognitive processes dependent on frontostriatal circuitry and contributes to multiple behavioral disorders associated with frontostriatal cognitive dysfunction (Broadbent 1971; Hartley and Adams 1974; Arnsten 2009; Hilton and Whiteford 2010). However, our understanding of the neural mechanisms that underlie the cognition-impairing effects of stress is limited, impeding our ability to better treat stress-related cognitive dysfunction. In nonhuman primates and rodents engaged in delayed-response tasks of working memory, subpopulations of PFC neurons have been identified that respond to key task events, including the delay interval and reward (Fuster and Alexander 1971; Goldman-Rakic 1995; Devilbiss et al. 2017). Similar task-dependent neurons are found within the striatum, including rodent dmSTR (Schultz and Romo 1988; Levy et al. 1997; Akhlaghpour et al. 2016; Hupalo et al. 2019). In earlier studies we observed that stress selectively suppresses the activity of putative dorsomedial PFC (dmPFC) pyramidal neurons tuned to delay and reward (Devilbiss et al. 2017). To date, the effects of stress on working memory-related activity of dmSTR neurons are unknown.

In addition to the activity of individual neurons, local field potential (LFP) oscillations and oscillatory synchrony between regions have been posited to coordinate information processing (Buzsaki 2010; Roux and Uhlhaas 2014). In terms of PFC-dependent cognition in humans, frontal cortex theta activity (4–7 Hz) is positively correlated with working memory performance (Gevins et al. 1997; Mitchell et al. 2008; Hsieh and Ranganath 2014), whereas stress-related impairment in working memory is associated with decreases in theta activity (Gartner et al. 2014). Alpha (8–12 Hz) and beta (15–35 Hz) activities in the PFC have also been positively associated with higher cognitive function, including working memory and inhibitory control (Klimesch 1999; Freunberger et al. 2011; Roux and Uhlhaas 2014). The sensitivity of these latter frequencies to stress is currently unknown. In contrast to the positive relationship between lower frequency oscillations and PFC-dependent cognition, stress was observed to increase PFC gamma power (40–80 Hz; Minguillon et al. 2016). In rodents, striatal oscillatory activity is also linked to a diversity of cognitive/behavioral processes (Berke et al. 2004; DeCoteau et al. 2007; van der Meer and Redish 2009). However, this latter work has generally not involved the dmSTR or cognitive tasks dependent on dorsomedial frontostriatal circuitry. Currently, we know little about the effects of stress on task-related oscillatory activity and oscillatory synchrony within the broader dorsomedial frontostriatal system, representing a significant gap

Received: November 11, 2022. **Revised:** February 22, 2023. **Accepted:** February 23, 2023

in our understanding of the neurobiology of both stress and higher cognitive function.

To address these issues, the current study examined the effects of working memory impairing acute noise-stress on single neuron spiking activity and spectral power within, and synchrony between, the dmPFC and dmSTR in rats engaged in a spatial working memory task.

Materials and methods

Subjects

Male Sprague–Dawley rats ($n = 13$, Charles River, Wilmington DE; 300–500 g) were housed individually with enrichment (Nylabone chews) and maintained on a 13/11-h light/dark cycle (lights on 0600 h) with ad lib water access. Food intake was limited to maintain motivation for food reward while avoiding weight loss (15–19 g chow per day). All procedures were in accordance with NIH and University of Wisconsin-Madison policies.

Working memory training

Animals were initially trained to perform a delayed non-match to position task as described previously (Devilbiss et al. 2012, 2017; Fig. 1). Briefly, animals were trained to enter the arm of a T-maze not chosen on the previous trial to receive food reward (one-half of a mini chocolate chip, 80 mg, Eilleen's Candies, Green Bay, WI, or 45 mg sucrose pellet/trial, Bio-Serv, Flemington, NJ). Distal visual cues were minimized with black plastic sheeting and the maze was wiped with 70% ethanol to minimize olfactory cues. Masking white noise (60 dB) was played above the center of the maze (Devilbiss et al. 2017). Initially, a testing session consisted of 10 trials. Between trials, animals were placed in a start box at the base of the maze and prevented from exiting by a gate that was removed at the end of the delay period. On the first trial preceding the 10 trials, animals could choose either arm. Animals were considered trained when they reached an average accuracy of 80% for 2 consecutive sessions, each consisting of 10 trials with a 0-s delay between trials.

Once trained, animals were implanted with recording electrodes and allowed to recover 7–10 days with ad lib feeding (Fig. 1). Prior studies demonstrate the targeted region of the dmSTR receives direct projections from the dmPFC and is necessary for successful performance in this task (Spencer et al. 2012; Spencer and Berridge 2019). Following recovery from surgery, mild food restriction was reinstated and animals were trained to perform 2 40-trial sessions per day (excluding the first trial), each separated by 2 h. Trials were separated initially by a 5-s delay. During training, animals were connected to a dummy headstage. When animals reached an average accuracy level of 80–95% across 2 testing days (no more than 10% variation across days), they were randomly assigned to white noise-stress (95 dB) or no-stress control conditions for the subsequent testing day. On the testing day, animals were connected to the recording headstage and then tested in a baseline session and 2 h later a second testing session either under no-stress control or noise-stress conditions. Between testing sessions, the headstage remained connected, allowing within-neuron analyses across testing sessions (see below). No-stress control was identical to baseline testing conditions (i.e. 60 dB white noise).

Surgery

Under isoflurane (Halocarbon Laboratories, River Edge, NJ), animals were stereotaxically implanted with 50 μm stainless-steel chronic recording electrodes targeting both the dmPFC and dmSTR, as previously described (Fig. 1; Devilbiss et al. 2012, 2017). In the dmPFC, an 8-wire linear electrode array (NB Labs, Dennison, TX) oriented along the rostral-caudal axis was positioned in layer V (centered at A/P +3.0 mm, M/L ±0.7 to 0.9 mm, D/V −2.5 to 3.0 m). In the dmSTR, a $2 \times 3 \times 3$ matrix electrode array (NB Labs, Dennison, TX) was implanted ipsilateral to the dmPFC electrodes (centered at A/P +0.45 mm, M/L ±3.5 mm with 11.5° angle, D/V −3.3 to 3.5 mm). Electrodes were secured with skull screws (MX-0080-16B-C, Small Parts, Inc., Logansport, IN) and dental acrylic (Plastics One, Roanoke, VA).

Testing and electrophysiological recording procedures

On testing days, animals were transported to the recording room and tethered to a 32-channel commutator and a multichannel electrophysiology acquisition processor (MAP, Plexon, Dallas, TX). Neural activity was amplified, discriminated, and time stamped (Devilbiss et al. 2017). Putative single units in the dmPFC and dmSTR exhibiting a ~3:1 signal-to-noise ratio were isolated (Fig. 1). The following measures were used to ensure that sorted waveforms arose from single neurons and remained stable throughout a testing session: (i) variability of peak waveform voltage, (ii) variability of waveform slope, (iii) scattergram distribution in the first 3 principal components, and (iv) refractory period (Fig. 1).

After spike-sorting, a 40-trial baseline recording session was conducted at ~11 AM, followed 2 h later by a second 40-trial session. During the second recording session, animals were tested either under conditions identical to baseline testing (*no-stress control*) or in the presence of 95 dB white noise (*stress*; Devilbiss et al. 2017). For animals exposed to noise-stress, the stressor was initiated immediately prior to and continued throughout the second session. This stressor is well documented to impair PFC-dependent cognition in humans, monkeys, and rodents (Arnsten et al. 1985; Becker et al. 1995; Arnsten and Goldman-Rakic 1998; Davis and Whalen 2001; Holmes and Wellman 2009; Szalma and Hancock 2011; Devilbiss et al. 2017) and, importantly, can be used concurrently with cognitive testing. Animals remained in the home cage and connected to the headstage between testing sessions. Analyses described above ensured stability of single-unit recordings throughout both testing sessions. Video recordings (80 frames/s) and IR beams were used to timestamp the animal's location in the T-maze (Fig. 1; see Devilbiss et al. 2017).

Given performance in this task improves over multiple testing sessions, when animals exceeded the 80–95% performance criterion, delay duration was increased in 5–10-s increments. The maximal delay duration used in these studies was 40 s. Animals were tested with noise-stress no more than once a week. Data from 3 animals were excluded from analyses because they were not behaviorally impaired by more than 10% during a second exposure to the stressor. Three animals were also excluded from data analyses because of failure to run the task during stress. For these latter animals, failure to run was observed on the first stress testing session and on a subsequent session.

Neuron identification and event tuning

For the dmPFC, wide-spiking (WS), putative glutamatergic pyramidal vs. narrow-spiking (NS), putative inhibitory interneuron cell types were differentiated based on trough-to-peak average of the waveform (WS > 200 μs; NS, 100–200 μs; Mitchell et al. 2007). For the dmSTR, medium spiny neurons (MSNs) and fast-spiking (FS) interneurons were identified using the peak-to-valley duration (MSN > 250 μs; FS < 200 μs). Because of a limited number

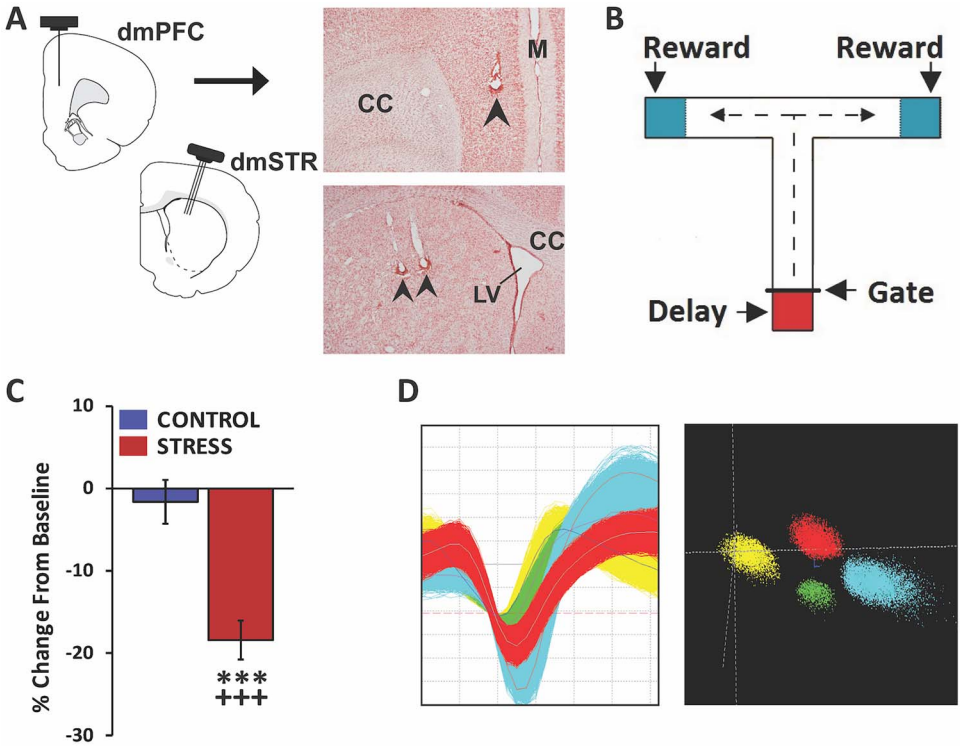

Fig. 1. Experimental approach. A) Schematic depicting 8-wire recording ensembles simultaneously targeting layer V of the dmPFC and the dmSTR. Accurate placement was confirmed in stained tissue sections. Photomicrograph of a coronal section demonstrating recording sites in dmPFC (top panel) and dmSTR (bottom panel). Arrows indicate recording electrodes tip location. CC, corpus collosum; LV, lateral ventricle; M, midline. B) Schematic of the delayed-response T-maze testing apparatus. Between trials, the animal is held in the start box (red shading) for a delay interval. Animal exit during the delay is prevented by a removeable gate. At the end of a successful trial the animal receives a reward (blue shading) before it is picked up and placed back in the start box. C) Animals were connected to a headstage and recorded for a baseline testing session in the morning and, in the afternoon, either a no-stress control session or noise-stress testing session. The headstage remained connected across morning and afternoon testing sessions. When tested under no-stress control conditions (control), working memory performance accuracy did not differ significantly from baseline. In contrast, stress significantly impaired performance, relative to baseline and no-stress controls. D) Left: action potential waveforms of 4 discriminated WS dmPFC neurons from a single wire. Right: waveforms from these units exhibit separable clusters in 3D-principal component space. Analyses ensured the same neurons were recorded across baseline and stress or no-stress testing sessions. $^{***}P < 0.001$ vs. no-stress controls; $^{+++}P < 0.001$ vs. baseline.

of NS dmPFC neurons and FS dmSTR interneurons identified, all subsequent analyses focused on WS PFC and MSN dmSTR neurons.

Distinct subpopulations of dmPFC and dmSTR neurons displayed excitatory responses to specific task events, including delay and reward (Figs. 2 and 3). Given high baseline task accuracy (control: 90.2 ± 1.5%; stress: 93.6 ± 1.0%; combined: 92.0 ± 0.9%), error responses of neurons could not be analyzed. Within both the dmPFC and dmSTR a relatively small number of neurons responded in a brief and time-locked manner to reward receipt. Instead, larger populations were observed that displayed a more sustained activation that began shortly prior to the physical receipt of reward, signaled by movement of the experimenter's hand toward the animal. These are referred to as "reward proximity" neurons and may reflect positive response outcome or reward anticipation rather than the hedonic experience of the reward. Neurons "strongly tuned" to task events were identified by calculating the z-score of firing rate during the relevant baseline interval vs. activity in a 14-s interval surrounding the task interval. Delay-tuned neurons were identified by a z-score > 0.07 and a baseline firing rate > 0.5 Hz, whereas reward proximity neurons were identified by a z-score > 0.2 and a baseline firing rate > 0.5 Hz. The longer duration of the delay interval warranted a smaller z-score. Units were considered outliers if the percent change from baseline was >3 median absolute deviations. This was typically associated with low baseline firing rates and resulted in the exclusion of 1–2 neurons per group. This approach identified neurons with response properties similar to those described by others (Fuster and Alexander 1971; Batuev et al. 1990; Goldman-Rakic 1995; Horst and Laubach 2009). Units not meeting these criteria were considered "untuned" to task events.

Local field potential analyses: spectral density and coherence

LFPs were recorded from all electrodes in the dmPFC and dmSTR (MAP, Plexon). For each recording day, one wire/region was selected for analysis, based on recording quality (power of signal and minimal noise). Signals were referenced to ground, amplified, filtered, and digitized at 1 kHz, then down sampled to 200 Hz. Stationarity of the LFP was enforced across trials and time via a z-score transformation combined with differencing the timeseries across time, resulting in the spectrum scaling as a function of frequency (Oppenheim and Schafer 1989). LFP spectral density was analyzed using continuous wavelet transform (cwtft, MATLAB), with Morlet wavelets, and logarithmically increasing frequency from 4 to 100 Hz. The absolute power at each frequency was then calculated by squaring the absolute value of the wavelet coefficient (Cohen 2014). Average power within distinct frequency bands (theta 4–7 Hz; alpha 7–12 Hz; beta 15–35 Hz; gamma 40–80 Hz) was calculated for each trial over the interval of interest.

To quantify synchrony, the cross-correlation as a function of frequency and time, wavelet transform coherence (wcoherence, MATLAB) with Morlet wavelets was calculated. Average synchrony per frequency band was calculated per trial.

Histology

Animals were deeply anesthetized and cathodal current (15 μA) was passed through each electrode for 10 s. Animals were then perfused with a 10% formalin solution. Brains were then removed, and immersed in 10% formalin for at least 24 h. Following fixation, brains were frozen and 40 μm coronal sections were collected through the dmPFC and dmSTR and stained with Neutral Red dye (Thermo Fisher Scientific, Waltham, MA).

Statistical analyses

Data were included only when histology verified accurate electrode placement and minimal tissue damage. Behavioral and electrophysiological measures were analyzed using a 2-way linear mixed-effects model, with session (baseline vs. treatment) and treatment (no-stress vs. stress) as fixed effects factors (JMP Pro Version 12.2.0, SAS Institute). When appropriate, pairwise comparisons of each group's change from its own baseline were determined using Tukey HSD. For working memory performance, we analyzed the average working memory performance across each 40-trial testing session. For single unit activity, the mean spiking rate during task intervals was determined on a trial-by-trial basis using peri-event time histogram (PETH) analysis, with 8 independent analyses per combination of region (dmPFC or dmSTR), interval (delay or reward proximity), and neuronal tuning (tuned or untuned). For LFP recordings, the trial-by-trial LFP spectral density was analyzed as described above, with independent analyses done on region (dmPFC or dmSTR), interval (delay or reward proximity), and frequency band (theta, alpha, beta, and gamma). Trial-by-trial coherence was analyzed as described above with independent analyses done on task interval and frequency band.

Results

We previously characterized the effects of noise-stress on delay- and reward-related activity of individual dmPFC neurons (Devilbiss et al. 2017). A subset of 5 animals from this prior study was used to pilot simultaneous dmPFC–dmSTR recordings during stress. For the current study we revised methods used to identify and analyze task-related single unit activity, including: (i) determining neuronal tuning from baseline trials only, (ii) the use of reward-proximity interval rather than reward receipt, and (iii) statistical analyses that include the interaction of treatment and session, rather than treating each manipulation independently. Given these changes, and to minimize animal use, we included dmPFC single unit data from the 5 animals with dual dmPFC–dmSTR recordings from our prior study.

Effects of stress on working memory performance

Under baseline conditions animals displayed high task performance accuracy (92.0 ± 0.9% correct, range 82.5–100% correct). As shown in Fig. 1, noise-stress, initiated at the start of the second testing session ($n = 16$), significantly impaired working memory performance accuracy relative to both baseline ($P < 0.0001$) and no-stress control (treatment $F_{(1,17.2)} = 3.04$, $P = 0.099$; session $F_{(1,28)} = 33.29$, $P < 0.0001$; treatment × session $F_{(1,28)} = 23.91$, $P < 0.0001$). In contrast, performance did not differ significantly from baseline under no-stress control testing conditions ($n = 14$; $P = 0.930$).

Effects of stress on task-related activity of dmPFC neurons

For dmPFC recordings, all electrodes were localized to layer V. Of the 343 recorded WS neurons identified, 57 (16.6%) were classified as strongly tuned to delay (Fig. 2). An additional 35 (10.5%) were identified as strongly tuned to reward proximity (Fig. 2). Only 2 neurons were strongly tuned to both events (3.5% of delay, 5.7% of reward proximity). Only 1 neuron displayed brief and time-locked responses to the physical receipt of food reward in the absence of reward-proximity activity and was excluded from analyses. The remaining neurons were classified as "untuned" to these task events.

Delay-related spiking activity of dmPFC neurons

As shown in Fig. 2, for *delay-tuned* neurons, noise-stress elicited a robust suppression of delay-related spiking activity of dmPFC neurons relative to baseline ($P < 0.0001$) and no-stress control (control, $n = 21$; stress, $n = 36$; treatment $F_{(1,55)} = 4.90$, $P = 0.031$; session $F_{(1,4501)} = 77.22$, $P < 0.0001$; treatment × session $F_{(1,4501)} = 69.51$, $P < 0.0001$). In contrast, under no-stress control conditions spiking activity of delay-tuned WS dmPFC neurons did not differ from baseline conditions ($P = 0.992$). For neurons that were *not tuned* to the delay interval, stress significantly *increased* delay-related firing relative to baseline ($P < 0.0001$) and no-stress control (Fig. 2; control, $n = 122$; stress, $n = 164$; treatment $F_{(1,284)} = 29.49$, $P < 0.0001$; session $F_{(1,22592)} = 43.53$, $P < 0.0001$; treatment × session $F_{(1,22592)} = 4.06$, $P = 0.044$). Delay-related activity of neurons not tuned to delay was moderately increased under no-stress control conditions relative to baseline ($P = 0.013$).

Reward-related spiking activity of dmPFC neurons

As shown in Fig. 2, stress also suppressed the spiking activity of dmPFC neurons tuned to reward proximity relative to baseline ($P < 0.0001$) and no-stress control (control, $n = 16$; stress, $n = 19$; treatment $F_{(1,33)} = 9.53$, $P = 0.004$; session $F_{(1,2319.6)} = 20.05$, $P < 0.0001$; treatment × session $F_{(1,2319.6)} = 6.31$, $P = 0.012$). Spiking activity of reward proximity-tuned dmPFC neurons did not differ from baseline under no-stress conditions ($P = 0.483$). The activity of dmPFC neurons not tuned to reward proximity significantly increased during that interval under no-stress control conditions relative to baseline (Fig. 2; $n = 127$; $p \leq 0.0001$). In contrast to that seen during the delay interval, stress significantly suppressed the activity of these neurons relative to no-stress control ($n = 171$; $F_{(1,296.4)} = 12.66$, $P = 0.0004$; session $F_{(1,19884)} = 17.69$, $P < 0.0001$; treatment × session $F_{(1,19884)} = 23.17$, $P < 0.0001$), but not relative to baseline ($P = 0.97$).

Effects of stress on task-related activity of dmSTR MSNs

As with the dmPFC, and as shown in Fig. 3, a relatively large population of MSNs was observed to be strongly tuned to delay ($n = 71$, 20.5%), whereas a smaller population was strongly tuned to reward proximity ($n = 25$, 7.7%). Only a minimal number of neurons displayed a brief and time-locked response to food reward receipt ($n = 3$, 0.86%) and were excluded from the analyses.

Delay-related spiking activity of dmSTR neurons

As shown in Fig. 3, stress elicited a robust suppression of *delay-tuned* MSN dmSTR neurons relative to baseline ($P < 0.0001$) and no-stress control (control, $n = 39$; stress, $n = 32$; treatment $F_{(1,69)} = 0.15$,

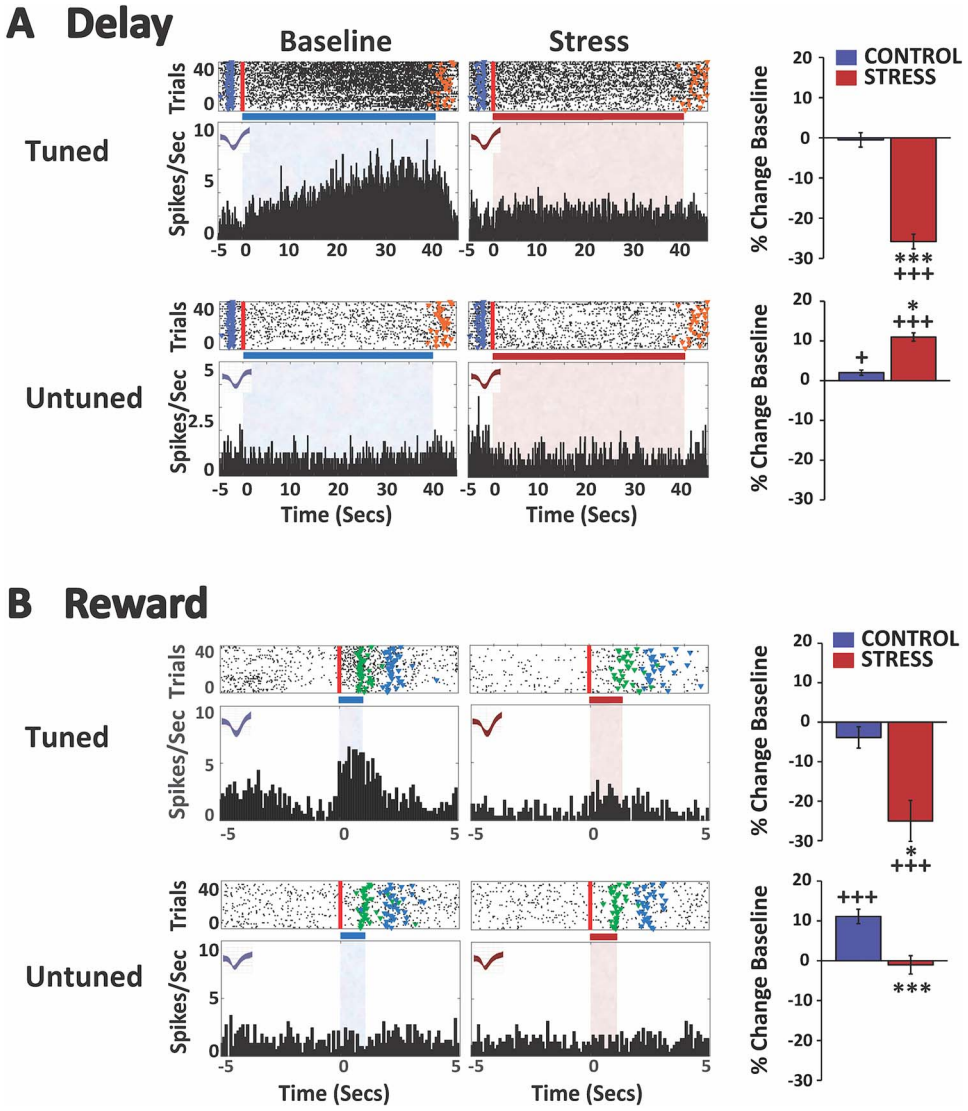

Fig. 2. Stress suppresses spiking activity of delay- and reward-tuned WS/pyramidal-dmPFC neurons. A) Stress suppresses *delay-related* activity of strongly tuned dmPFC neurons. *Top row*: spike rasters and PETHs of a single exemplar neuron strongly tuned (tuned) to the delay interval under both baseline and stress conditions (no-stress control rasters/PETHs not shown). In raster displays, vertical red line indicates start of the delay interval and colored fiducial markers indicate beginning of additional events: blue, pickup; orange, gate lift (end of delay). Horizontal bar and shading (blue, baseline; red, stress) indicate delay interval. *X*-axes = time (s), *Y*-axes = spiking frequency. Bar graphs depict mean change (±SEM) from baseline firing rate of all neurons classified as strongly tuned to the delay interval. For neurons strongly tuned to delay, stress significantly suppressed delay-related firing relative to baseline and no-stress controls. *Bottom row*: spike rasters and PETHs of a single neuron not tuned (untuned) to delay under baseline and stress conditions. Stress significantly increased delay-related firing for untuned neurons relative to baseline and no-stress controls (bar graphs). B) Stress suppresses *reward-related* activity of strongly tuned dmPFC neurons. *Top row*: spike rasters and PETHs of a single neuron strongly tuned to the reward interval under baseline and stress conditions (only correct trials on which reward was received are plotted/analyzed). In raster displays, vertical red line indicates start of the reward proximity interval and colored fiducial markers indicate beginning of additional events: green, sugar reward receipt; blue, pickup. Bar graphs indicate stress significantly suppressed reward-related firing in this population of neurons relative to baseline and no-stress controls. *Bottom row*: spike rasters and PETHs of a single neuron not tuned to reward under baseline and stress conditions. In no-stress controls, there was a modest increase in reward-related firing of untuned neurons during the second testing session. Stress significantly suppressed reward-related activity relative to no-stress controls. $^{*}P < 0.05$, $^{***}P < 0.001$ vs. no-stress control. $^{+}P < 0.05$, $^{+++} < 0.001$ vs. baseline.

$P = 0.697$; session $F_{(1,5607)} = 72.38$, $P < 0.0001$; treatment × session $F_{(1,5607)} = 66.87$, $P < 0.0001$). The magnitude of this suppression was comparable to that seen in the dmPFC. Under no-stress control conditions, spiking activity of delay-tuned dmSTR neurons did not differ from the baseline testing session ($P = 0.995$). For MSNs *not tuned* to the delay interval, stress had no significant effects on delay-related firing relative to baseline ($P = 0.222$) or no-stress control (Fig. 3; control, $n = 109$; stress, $n = 167$; treatment $F_{(1,274)} = 6.38$, $P = 0.012$; session $F_{(1,21802)} = 2.82$, $P = 0.093$; treatment × session $F_{(1,21802)} = 0.53$, $P = 0.467$). Under no-stress control conditions, delay-related spiking activity of dmSTR neurons not tuned to the delay interval did not differ across the baseline and testing sessions ($P = 0.928$).

Reward-related spiking activity of dmSTR neurons

Stress also suppressed the firing rate of MSN dmSTR neurons tuned to reward proximity relative to baseline ($P = 0.001$) and no-stress control (Fig. 3; control, $n = 11$; stress, $n = 14$; treatment $F_{(1,23)} = 0.19$, $P = 0.666$; session $F_{(1,1580.3)} = 6.45$, $P = 0.011$; treatment × session $F_{(1,1580.3)} = 7.28$, $P = 0.007$). The magnitude of this

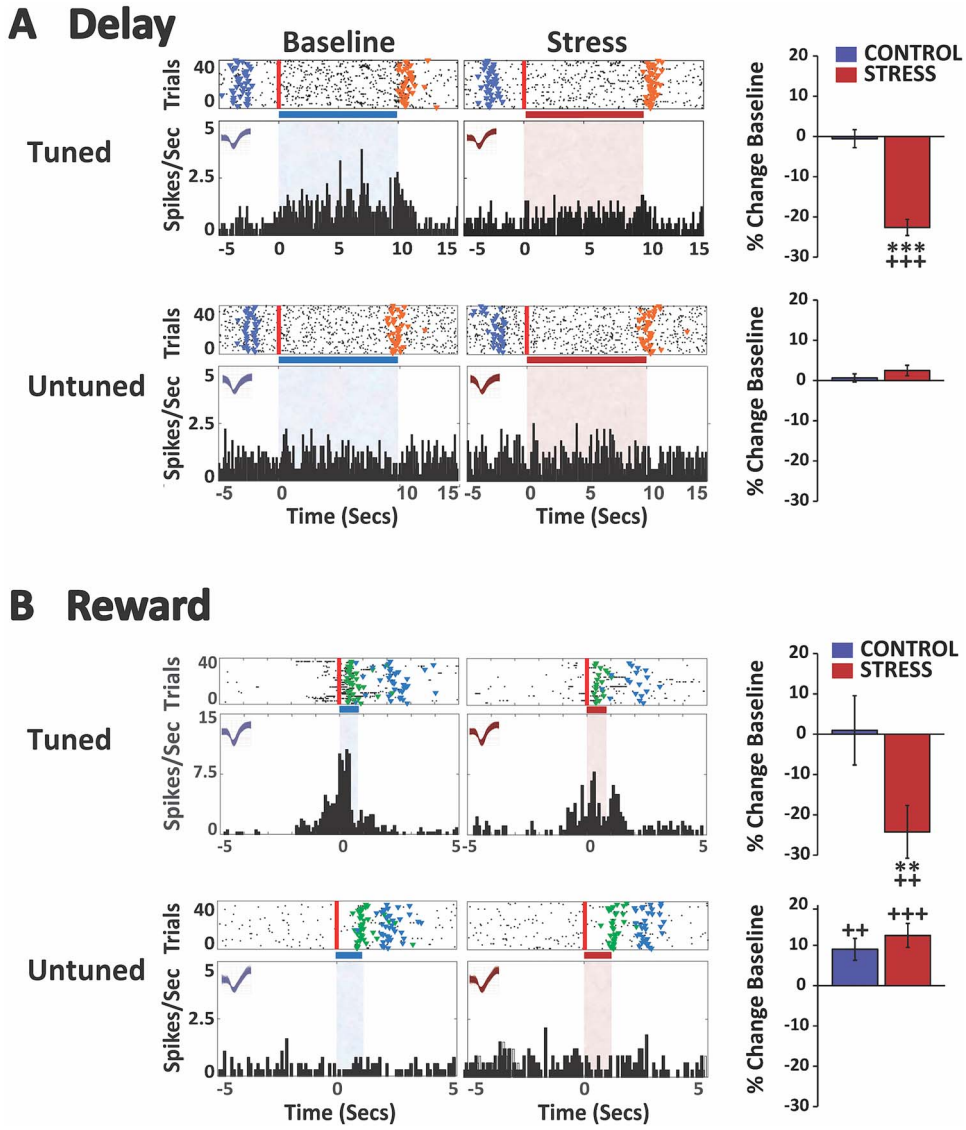

Fig. 3. Stress suppresses spiking activity of delay- and reward-tuned dmSTR MSNs. A) Stress suppresses *delay-related* activity of strongly tuned dmSTR neurons. *Top row*: spike rasters and PETHs of a single neuron strongly tuned to the delay interval under baseline and stress conditions (no-stress control rasters/PETHs not shown). In raster displays, vertical red line indicates start of the delay interval and colored fiducial markers indicate beginning of additional events: blue, pickup; orange, gate lift (end of delay). Horizontal bar and shading (blue, baseline; red, stress) indicate delay interval . *X*-axes = time (s), *Y*-axes = spiking frequency. Bar graphs depict mean change (±SEM) from baseline firing rate of all neurons classified as strongly tuned to the delay interval. For neurons strongly tuned to delay, stress significantly suppressed delay-related firing relative to baseline and no-stress controls. *Bottom row*: spike rasters and PETHs of a single dmSTR neuron not tuned to delay under baseline and stress conditions. Stress did not affect delay-related firing for neurons not tuned to delay. B) Stress suppresses *reward-related* activity of strongly tuned dmSTR MSNs. *Top row*: spike rasters and PETHs of a single neuron strongly tuned to the reward interval under both baseline and stress conditions (only correct trials on which reward was received are plotted/analyzed). In raster displays, vertical red line indicates start of the reward proximity interval and colored fiducial markers indicate beginning of additional events: green, sugar reward receipt; blue, pickup. Stress significantly decreased the firing rate of reward-tuned dmSTR MSNs relative to baseline and no-stress controls. *Bottom row*: spike rasters and PETHs of a single MSN neuron not tuned to reward under both baseline and stress conditions. In no-stress controls, there was a modest increase in reward-related firing rate of untuned neurons during the second testing session. Stress did not significantly affect this. $^{**}P < 0.01$, $^{***}P < 0.001$ vs. no-stress control. $^{++}P < 0.01$, $^{+++}P < 0.001$ vs. baseline.

suppression was comparable to that seen in the PFC. Under no-stress control conditions, proximity reward-related spiking activity of dmSTR neurons did not differ from baseline ($P = 0.999$). As with the PFC, the activity of MSNs *not tuned* to reward proximity increased modestly, but significantly, under no-stress testing conditions relative to baseline (Fig. 3; $n = 133$; $P = 0.005$). However, unlike in the dmPFC, stress did not significantly change this effect relative to no-stress control ($n = 166$; treatment $F_{(1,297.5)} = 0.49$, $P = 0.484$; session $F_{(1,19793)} = 28.15$, $P < 0.0001$; treatment × session $F_{(1,19793)} = 0.24$, $P = 0.624$).

Effects of stress on frontostriatal oscillatory power

The effects of stress on spectral power in the dmPFC and dmSTR during the delay and reward proximity intervals of the working memory task were also examined (control: $n = 14$; stress: $n = 12$). Under baseline conditions during the delay (Fig. 4) and reward proximity (Fig. 6) intervals, a dominant peak was observed centered at 8 Hz that spanned both theta (4–7 Hz) and alpha frequency bands (7–12 Hz). A second and broad peak, which included beta (15–35 Hz) and gamma (40–80 Hz) frequencies, was also seen

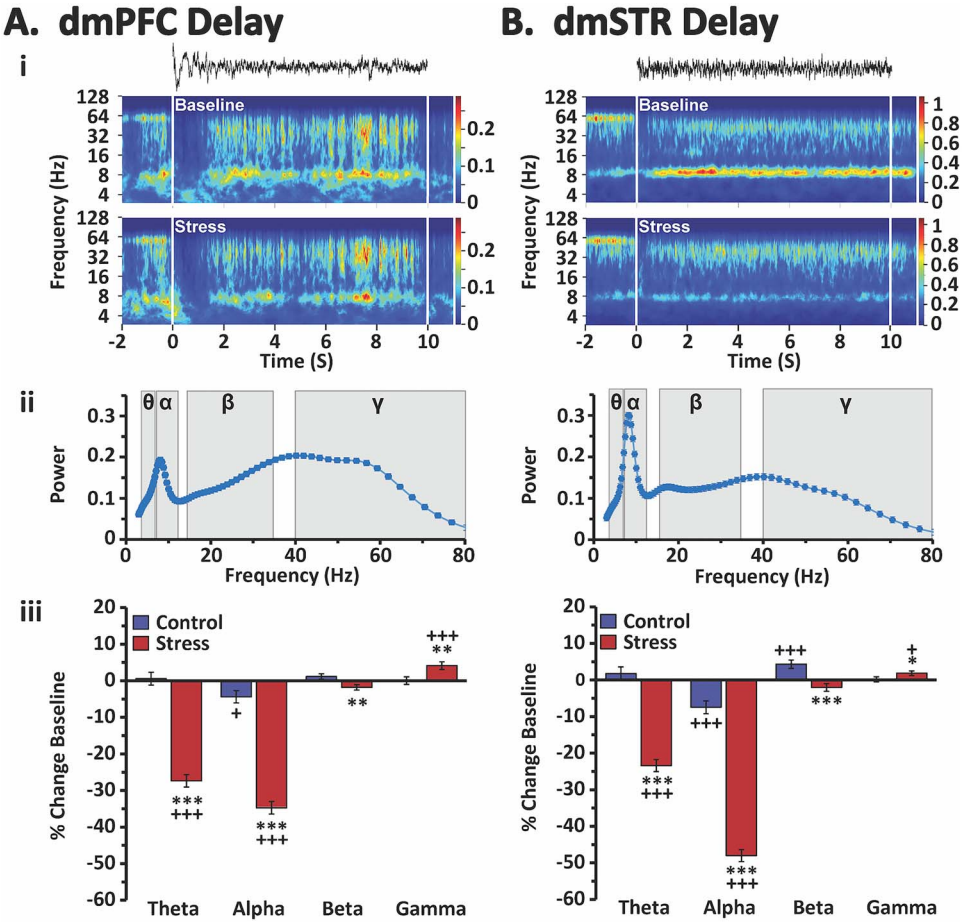

Fig. 4. Stress effects on delay-related oscillatory activity in the dmPFC and dmSTR. Shown are analyses of delay-related LFP oscillatory activity in the dmPFC A) and dmSTR B). i) Raw LFP recording traces during a 10-s delay interval of a single trial (top) and time-frequency spectrograms for the delay interval averaged across all trials of an individual animal during both baseline (middle) and stress (bottom) recording sessions. White vertical lines indicate beginning and end of the delay interval. Color scale bar reflects absolute power of LFP. ii) Spectral density plots of mean power for all animals during the delay interval of baseline testing (4–80 Hz). Shading indicates theta (θ), alpha (α), beta (β), and gamma (γ) frequencies. Under baseline conditions there was a peak spanning theta and alpha frequencies, reaching a maximum at ~8 Hz (low alpha) followed by a broader peak that reached a maximum at low gamma. iii) Percent change in power (± SEM) from baseline during the delay interval for each analyzed frequency band for stress and no-stress control animals. Stress robustly suppressed delay-related theta and alpha power, while modestly suppressing beta activity, in both the dmPFC and dmSTR. Conversely, stress elicited a small, yet significant increase in delay-related gamma power in both regions. $^{*}P < 0.05$, $^{**}P < 0.01$, $^{***}P < 0.001$ vs. no-stress control. $^{+}P < 0.05$, $^{+++}P < 0.001$ vs. baseline.

throughout both intervals. This was most prominent in the dmPFC during delay and smallest in the dmSTR during reward proximity.

Stress and delay-related oscillatory activity

Stress robustly suppressed delay-related theta and alpha power in both the dmPFC and the dmSTR relative to baseline and no-stress control (Fig. 4; see Table 1 for statistical analysis results). No change in theta power was observed under no-stress control conditions in either the dmPFC or the dmSTR. However, there was a small, but significant, decrease in alpha power during the no-stress control session in both the dmPFC and the dmSTR relative to baseline. Stress elicited a weaker, but significant, suppression of delay-related beta power in the dmPFC and dmSTR relative to no-stress control, but not baseline (Fig. 4; see Table 1 for statistical results). However, in visual examination of the spectral density plots, stress appeared to differentially impact lower (15–25 Hz) vs. higher (25–35 Hz) beta frequencies during delay. Additional analyses demonstrated that stress significantly decreased delay-related low beta power, while significantly increasing higher beta power in both the dmPFC and dmSTR (Fig. 5). Stress also increased delay-related gamma power in the dmPFC and dmSTR relative to baseline and no-stress control (Fig. 4 and Table 1).

Thus, stress differentially affects lower vs. higher frequencies in both the dmPFC and dmSTR during the delay period. Stress-related changes in delay-related theta/alpha power were notably larger than stress-related increases in high-beta and gamma.

Stress and reward-related oscillatory activity

In contrast to that seen for delay, reward proximity-related oscillatory activity in the dmPFC was largely insensitive to stress (Fig. 6 and Table 1). The one exception was a small, yet significant, increase in reward-related gamma power. Under no-stress control conditions, there were no significant changes in reward-related spectral power within the dmPFC.

Within the dmSTR, neither no-stress control nor stress conditions affected reward-related oscillatory activity in any frequency band (Fig. 6 and Table 1).

Effects of stress on frontostriatal oscillatory synchrony

Delay-related synchrony

Under baseline conditions, there was a peak of dmPFC–dmSTR coherent theta and alpha activity during delay (Fig. 7). Stress

Table 1. Statistical analyses for delay- and reward-related oscillatory activity.

Interval	Frequency	Source	dmPFC	dmSTR
Delay	Theta	TRT	$F_{1,18.1} = 0.41$, $P = 0.528$	$F_{1,16.5} = 0.62$, $P = 0.441$
		SESS	$F_{1,2052} = 138.03$, $P < 0.0001$	$F_{1,2052} = 94.27$, $P < 0.0001$
		TRT*SESS	$F_{1,2052} = 148.31$, $P < 0.0001$	$F_{1,2052} = 121.72$, $P < 0.0001$
	Alpha	TRT	$F_{1,15.9} = 3.05$, $P = 0.100$	$F_{1,16.1} = 1.26$, $P = 0.278$
		SESS	$F_{1,2052} = 275.25$, $P < 0.0001$	$F_{1,2052} = 592.1$, $P < 0.0001$
		TRT*SESS	$F_{1,2052} = 169.88$, $P < 0.0001$	$F_{1,2052} = 344.32$, $P < 0.0001$
	Beta	TRT	$F_{1,15.7} = 1.37$, $P = 0.259$	$F_{1,15.6} = 2.13$, $P = 0.164$
		SESS	$F_{1,2052} = 0.61$, $P = 0.435$	$F_{1,2052} = 1.38$, $P = 0.241$
		TRT*SESS	$F_{1,2052} = 7.86$, $P = 0.005$	$F_{1,2052} = 16.18$, $P < 0.0001$
	Gamma	TRT	$F_{1,14.9} = 0.87$, $P = 0.366$	$F_{1,14.9} = 4.65$, $P = 0.048$
		SESS	$F_{1,2052} = 8.13$, $P = 0.004$	$F_{1,2052} = 5.87$, $P = 0.016$
		TRT*SESS	$F_{1,2052} = 7.85$, $P = 0.005$	$F_{1,2052} = 4.18$, $P = 0.041$
Reward	Theta	TRT	$F_{1,16.5} = 6.96$, $P = 0.018$	$F_{1,17.6} = 0.94$, $P = 0.346$
		SESS	$F_{1,1760.8} = 0.99$, $P = 0.321$	$F_{1,1760.8} = 0.57$, $P = 0.449$
		TRT*SESS	$F_{1,1761.9} = 0.70$, $P = 0.403$	$F_{1,1761.9} = 0.10$, $P = 0.757$
	Alpha	TRT	$F_{1,16.4} = 9.40$, $P = 0.007$	$F_{1,16.8} = 3.23$, $P = 0.090$
		SESS	$F_{1,1753.8} = 4.58$, $P = 0.033$	$F_{1,1752.4} = 4.76$, $P = 0.029$
		TRT*SESS	$F_{1,1754.5} = 0.06$, $P = 0.799$	$F_{1,1752.9} = 0.53$, $P = 0.466$
	Beta	TRT	$F_{1,15.1} = 4.98$, $P = 0.041$	$F_{1,16.1} = 0.58$, $P = 0.458$
		SESS	$F_{1,1750} = 0.45$, $P = 0.501$	$F_{1,1748.9} = 0.02$, $P = 0.889$
		TRT*SESS	$F_{1,1750.4} = 0.13$, $P = 0.719$	$F_{1,1749.1} = 2.17$, $P = 0.141$
	Gamma	TRT	$F_{1,15.2} = 0.81$, $P = 0.381$	$F_{1,15} = 0.16$, $P = 0.695$
		SESS	$F_{1,1748.6} = 2.07$, $P = 0.150$	$F_{1,1748} = 0.68$, $P = 0.411$
		TRT*SESS	$F_{1,1748.8} = 6.52$, $P = 0.011$	$F_{1,1748.2} = 0.02$, $P = 0.879$

Results of 2-way mixed model statistical analyses of local field potential recordings within the dorsomedial PFC (dmPFC) and dorsomedial striatum (dmSTR) during the delay and reward intervals across the 4 analyzed frequency bands: theta, alpha, beta, and gamma. TRT, treatment (stress vs. no-stress control); SESS, session (baseline vs. second testing session).

significantly decreased delay-related theta and alpha synchrony relative to baseline and no-stress controls (Fig. 7 and Table 2). In contrast, stress elicited a small, yet significant, increase in dmPFC–dmSTR beta synchrony, which was largely driven by increased coherence in the higher beta frequencies (data not shown). Stress had no effect on delay-related gamma synchrony. In no-stress controls, delay-related dmPFC–dmSTR synchrony was not affected in any of the frequency bands relative to baseline.

Reward-related synchrony

We also observed a peak of dmPFC–dmSTR theta and alpha synchrony during the reward-proximity interval during baseline (Fig. 7). However, unlike delay, stress had no significant effects on reward-related dmPFC–dmSTR synchrony in any frequency band (Fig. 7 and Table 2). During no-stress control conditions, theta and gamma synchrony were unchanged during reward proximity. However, there were reductions in alpha and beta synchrony in no-stress controls, neither of which were observed under stress conditions. Nonetheless, there were no significant differences in alpha or beta synchrony between stress and no-stress controls.

Discussion

Successful goal attainment requires the maintenance of information in the absence of sensory cues combined with the development and updating of action plans, often while confronting distractors and/or ambiguity. Frontostriatal circuits support a diversity of "executive" cognitive processes that support goal attainment. Stress impairs frontostriatal cognitive function, an action with strong relevance for health and safety (Broadbent 1971; Arnsten 2009). However, our understanding of the neurobiology underlying stress-related impairment in frontostriatal cognitive function is limited. To date, the majority of research in this area has focused on the PFC (Arnsten 2009; Devilbiss et al. 2017). Despite extensive evidence demonstrating a critical role of the dmSTR in "PFC-like" higher cognitive function, the impact of stress on this region has been overlooked. The current studies demonstrate that stress strongly disrupts working memory-related neural coding and functional connectivity within this cognition-supporting dorsomedial frontostriatal pathway. At the level of oscillatory activity and oscillatory synchrony, the effects of stress were largely limited to the delay interval. Collectively, these actions may contribute to stress-related impairment in higher cognitive function and stress-related psychopathology associated with impaired PFC-dependent cognition.

Effects of stress on task-related activity of individual neurons

At the single neuron level, stress robustly suppressed spiking activity of neurons strongly tuned to delay and reward in both the dmPFC and dmSTR. In both regions, there were larger populations of neurons tuned to delay than impending reward (reward proximity). Thus, delay-related neuronal activity within the dmPFC and dmSTR is a particularly prominent component of working memory performance. As observed previously (Devilbiss et al. 2017), stress resulted in an *activation* of the larger population of dmPFC neurons not tuned to delay, further degrading the population-level representation of information associated with delay. While dysregulated GABAergic transmission within the PFC has been observed in stress (McKlveen et al. 2016; Page and Coutellier 2019; Ghosal et al. 2020), the current observations indicate stress does not simply modulate overall inhibitory or

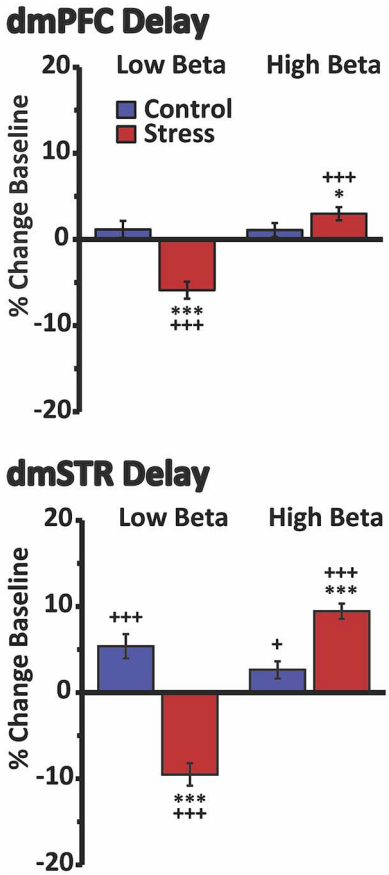

Fig. 5. Divergent effects of stress on delay-related low- vs. high-beta in the dmPFC and dmSTR. Shown are the percent change in power (±SEM) for low- (15–25 Hz) vs. high-beta (25–35 Hz) activity during the delay interval for stress and no-stress control animals. Within both the dmPFC (top) and dmSTR (bottom), stress elicited a modest, yet significant, suppression of delay-related low-beta oscillatory activity, while significantly increasing high-beta activity. $^{*}P < 0.05$ vs. no-stress control. $^{*}P < 0.05$, $^{***}P < 0.001$ vs. no-stress control. $^{+}P < 0.05$, $^{+++}P < 0.001$ vs. baseline.

excitatory tone within either the dmPFC or dmSTR. Instead, stress disrupts the encoding of key task-related information via complex actions across distinct subpopulations of neurons within these regions.

Stress increases catecholamine release in the PFC (Thierry et al. 1976; Dunn 1988; Abercrombie et al. 1989). The selective effect of stress on neurons strongly tuned to key task events is similar to that previously described for catecholamines in multiple regions, including the PFC (Berridge and Waterhouse 2003; Arnsten 2011). Of particular relevance, catecholamines exert an inverted-U shaped modulation of delay-related firing within the PFC, with higher rates of release engaging noradrenergic $\alpha 1$ and dopaminergic D1 receptors, resulting in a suppression of delay-related activity (Arnsten 2011). These observations suggest D1 and $\alpha 1$ receptors may participate in the degradative effects of stress on dmPFC neural coding.

The mechanisms responsible for stressor-induced suppression of task-related neuronal activity within the dmSTR are currently unclear. Given the dmPFC has direct, excitatory projections to the dmSTR, stressor-induced inhibition of task-related signaling of dmPFC neurons may well weaken task-related activity within the dmSTR. Stress also increases DA release within the dorsal striatum, although the magnitude of this is significantly less than seen in the PFC (Dunn 1988; Abercrombie et al. 1989). While stress-related elevations in DA could play a role in the neurophysiological actions of stress within the dmSTR, DA has been demonstrated to typically exert excitatory actions on striatal MSNs (Rebec et al. 1997; Surmeier et al. 2007). Beyond catecholamines, stressor-induced elevations in serotonin, glucocorticoids, or other neuromodulators could contribute to stress-related degradation of task-related spiking activity of dmSTR and dmPFC neurons.

Interestingly, while chronic stress was observed to decrease the activity of dmPFC neurons in animals tested in a cost–benefit conflict test, similar to that observed in the current study with acute stress, the opposite effect was observed for striosomal projection neurons in the dmSTR (Friedman et al. 2017). While the current study did not limit dmSTR recordings to striosomal projection neurons, these observations suggest the hypothesis that in contrast to acute stress, sustained exposure to stress may trigger neuroadaptations that results in disinhibition of the dmSTR.

Effects of stress on oscillatory activity within dorsomedial circuitry

At the level of LFPs, stress elicited event-, region-, and frequency-specific effects. The most robust of these was the suppression of delay-related theta (4–7 Hz) and alpha (7–12 Hz) spectral power within, and synchrony between, the dmPFC and dmSTR. Interestingly, this was not observed for reward proximity. The presence of delay-related theta and alpha activity in the dmPFC, as well as the sensitivity of this activity to stress, is consistent with prior observations in humans (Gevins et al. 1997; Klimesch 1999; Jensen and Tesche 2002; Bonnefond and Jensen 2012; Gartner et al. 2014; Manza et al. 2015; Popescu et al. 2016, 2019). Stress-related suppression of theta and alpha activity in the PFC could well contribute to an inability to maintain information over a delay period. While striatal oscillatory activity has been linked to a diversity of cognitive and behavioral processes (Berke et al. 2004; DeCoteau et al. 2007; van der Meer and Redish 2009), most of this research has not involved the dmSTR or working memory. The current studies provide the first demonstration that working memory performance is associated with a robust peak of theta and alpha activity in the dmSTR during both the delay and reward intervals. However, as with the PFC, stress potently suppressed delay-related, but not reward-related, theta and alpha power in the dmSTR as well as dmPFC–dmSTR theta/alpha synchrony. The differential sensitivity of delay- and reward-related theta/alpha activity suggests a prominent role of delay-related theta/alpha activity in the support of working memory as well as in the working memory impairing actions of stress. The suppression of delay-related theta/alpha synchrony in stress may reflect an impaired ability to maintain information flow between these regions necessary for successful task completion. This said, there was not a strong correlation between percent change in delay-related theta/alpha power or synchrony and percent change in task performance (data not shown). These latter observations could reflect the fact that oscillatory activity within this dorsomedial frontostriatal pathway is only one component of the neural architecture supporting higher cognitive function.

In contrast to the large suppressive actions of stress on theta and alpha activity, stress elicited relatively small increases in

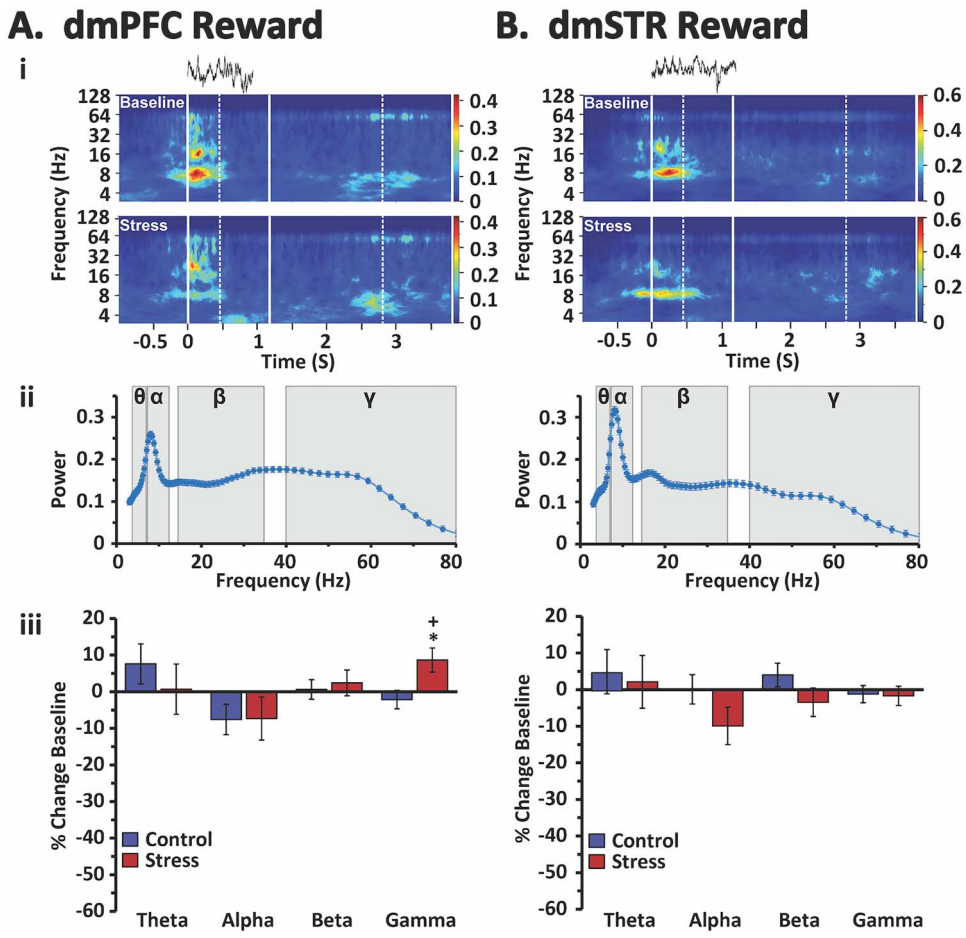

Fig. 6. Stress effects on reward-related oscillatory activity in the dmPFC and dmSTR. Shown are reward proximity-related analyses of LFP oscillatory activity in the dmPFC A) and dmSTR B). i) Raw LFP recording traces from a single trial (top) and the time-frequency spectrograms for the reward-proximity intervals averaged across all correct trials of an individual animal during both baseline (middle) and stress (bottom) recording sessions. Solid vertical white lines indicate the beginning of the interval (left-most solid line) and the average trial length (right-most solid line). Dotted vertical white lines indicate the minimum (left-most) and maximum (right-most) range of the reward-proximity interval. Color scale bar reflects absolute power of LFP. ii) Spectral density plots of mean power for all animals during the reward proximity interval of baseline testing (4–80 Hz), shading indicates theta (θ), alpha (α), beta (β), and gamma (γ) frequencies. Under baseline conditions there was a peak spanning theta and alpha frequencies, reaching a maximum at ~8 Hz (low alpha) followed by a broader peak that reached a maximum at low gamma. iii) Percent change in power (±SEM) from baseline during the reward proximity interval for each analyzed frequency band for stress and no-stress control animals. Stress had minimal effects on reward-related oscillatory activity, with the single exception being a small increase in gamma in the dmPFC. $^{*}P < 0.05$ vs. no-stress control. $^{+}P < 0.05$ vs. baseline.

higher frequency oscillations within the dmPFC and dmSTR, particularly during the delay interval. This is consistent with previously observed increases in frontal gamma power in a variety of mental illnesses associated with impaired PFC cognitive function, including PTSD, depression, and schizophrenia (Basar-Eroglu et al. 2007; Strelets et al. 2007; Moon et al. 2018). The neural mechanisms that underlie the differential actions of stress across task events and oscillatory frequencies are currently unclear. However, similar to that concluded for single-unit activity, these task- and frequency-selective effects of stress indicate that stress is not simply altering inhibitory or excitatory tone within this frontostriatal circuit to influence oscillatory activity.

It should be noted that studies in humans typically define theta as oscillations in the 4–7 Hz range, and alpha as being comprised of 7–12 Hz activity. In contrast, some studies in rodents have more broadly defined theta as spanning 4–12 Hz activity (Buzsaki 2005). Nonetheless, in other studies in rodents, 4–7 Hz and 7–12 Hz have been, respectively, referred to as type II vs. type I theta (Kramis et al. 1975; Vanderwolf and Robinson 1981), low vs. high theta (Cervera-Ferri et al. 2011; Mouchati et al. 2020), or theta vs. alpha (Tort et al. 2010). Interestingly, there appear to be functional and neurochemical differences between these distinct frequency ranges in rodents. In particular, 8–12 Hz oscillations are enhanced with locomotion and resistant to cholinergic manipulations, whereas 4–7 Hz activity is more prominent in immobile animals and eliminated by the muscarinic antagonist, atropine (Kramis et al. 1975; Vanderwolf and Robinson 1981). Taken together, this suggests that even in rodents, the broader 4–12 Hz frequency range supports distinct processes that can be differentiated across the 4–7 Hz and 7–12 Hz frequency bands, regardless of whether these are referred to as subcategories of theta or as theta vs. alpha.

Summary

The current studies demonstrate that stress impairs neural coding within a cognition-supporting frontostriatal pathway. This was observed for single neuron activity as well as at the level of

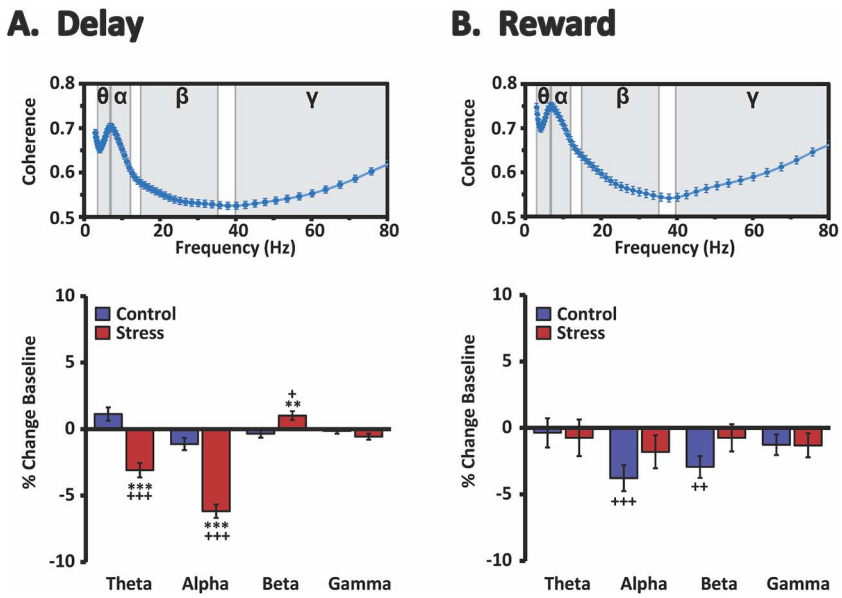

Fig. 7. Effects of stress on delay- and reward-related dmPFC–dmSTR oscillatory synchrony. *Top row*: shown are mean spectral coherence plots during the delay A) and reward B) intervals for all animals under baseline testing conditions. There was a prominent peak in spectral synchrony (coherence) spanning theta and alpha frequencies and reaching a maximum at ~7 Hz during both the delay a) and reward b) intervals. Shading indicates theta (θ), alpha (α), beta (β), and gamma (γ) frequencies. *Bottom row*: mean percent change (±SEM) from baseline under no-stress control and stress testing conditions. Stress significantly suppressed delay-related dmPFC–dmSTR theta and alpha synchrony while modestly increasing delay-related beta synchrony. Stress had no significant effects on reward-related synchrony. $^{**}P < 0.01$, $^{***}P < 0.001$ vs. no-stress control. $^{+}P < 0.05$, $^{++}P < 0.01$, $^{+++}P < 0.001$ vs. baseline.

Table 2. Statistical analyses for delay- and reward-related oscillatory synchrony between the dmPFC and dmSTR.

Interval	Frequency	Source	Results
Delay	Theta	TRT	$F_{1,17.4} = 0.60$, $P = 0.447$
		SESS	$F_{1,2052} = 7.01$, $P = 0.008$
		TRT*SESS	$F_{1,2052} = 32.75$, $P < 0.0001$
	Alpha	TRT	$F_{1,16.5} = 6.32$, $P = 0.023$
		SESS	$F_{1,2052} = 112.48$, $P < 0.0001$
		TRT*SESS	$F_{1,2052} = 52.87$, $P < 0.0001$
	Beta	TRT	$F_{1,15.7} = 1.20$, $P = 0.290$
		SESS	$F_{1,2052} = 2.17$, $P = 0.141$
		TRT*SESS	$F_{1,2052} = 9.09$, $P = 0.003$
	Gamma	TRT	$F_{1,15.1} = 0.01$, $P = 0.907$
		SESS	$F_{1,2052} = 5.24$, $P = 0.022$
		TRT*SESS	$F_{1,2052} = 1.99$, $P = 0.159$
Reward	Theta	TRT	$F_{1,17.9} = 1.63$, $P = 0.218$
		SESS	$F_{1,1721} = 0.39$, $P = 0.531$
		TRT*SESS	$F_{1,1721} = 0.04$, $P = 0.844$
	Alpha	TRT	$F_{1,17.4} = 2.04$, $P = 0.171$
		SESS	$F_{1,1720.8} = 12.91$, $P = 0.0003$
		TRT*SESS	$F_{1,1720.9} = 1.91$, $P = 0.167$
	Beta	TRT	$F_{1,18.4} = 0.80$, $P = 0.323$
		SESS	$F_{1,1720.5} = 8.17$, $P = 0.004$
		TRT*SESS	$F_{1,1720.6} = 3.06$, $P = 0.080$
	Gamma	TRT	$F_{1,16.9} = 0.05$, $P = 0.818$
		SESS	$F_{1,1720.4} = 4.66$, $P = 0.031$
		TRT*SESS	$F_{1,1720.5} = 0.002$, $P = 0.963$

Results of 2-way mixed model statistical analyses of synchrony between the dorsomedial PFC (dmPFC) and dorsomedial striatum (dmSTR) during the delay and reward intervals across the 4 analyzed frequency bands: theta, alpha, beta, and gamma.

oscillatory power and synchrony. In terms of oscillatory activity, the most robust effects of stress were the suppression of delay-related theta (4–7 Hz) and alpha (7–12 Hz) activity within and between the dmPFC and dmSTR. These results indicate that stress elicits task-, neuron-, and frequency-specific degradation in frontostriatal neural coding of higher cognitive function.

Author contributions

Craig Berridge (Conceptualization, Data curation, Formal analysis, Funding acquisition, Investigation, Methodology, Project administration, Resources, Supervision, Writing—original draft, Writing—review & editing), David M. Devilbiss (Conceptualization, Investigation, Methodology, Writing—review & editing), Andrea Martin (Data curation, Formal analysis, Investigation, Methodology, Project administration, Writing—review & editing), Robert Spencer (Methodology, Writing—review & editing), and Rick L. Jenison (Methodology, Writing—review & editing)

Funding

The National Science Foundation (IOS-0918555); the National Institutes of Health (MH081843, MH116526).

Conflict of interest statement: The authors declare no financial interests or potential conflicts.

Data availability

The datasets associated with this study are available from the corresponding author on reasonable request.

References

Abercrombie ED, Keefe KA, DiFrischia DS, Zigmond MJ. Differential effect of stress on in vivo dopamine release in striatum, nucleus accumbens, and medial frontal cortex. *J Neurochem*. 1989:52(5): 1655–1658.

Akhlaghpour H, Wiskerke J, Choi JY, Taliaferro JP, Au J, Witten IB. Dissociated sequential activity and stimulus encoding in the dorsomedial striatum during spatial working memory. *eLife*. 2016:5:e19507.

Arnsten AF. Stress signalling pathways that impair prefrontal cortex structure and function. *Nat Rev Neurosci*. 2009:10(6):410–422.

Arnsten AF. Catecholamine influences on dorsolateral prefrontal cortical networks. *Biol Psychiatry*. 2011:69(12):e89–e99.

Arnsten AF, Berridge C, Segal DS. Stress produces opioid-like effects on investigatory behavior. *Pharmacol Biochem Behav*. 1985:22(5): 803–809.

Arnsten AF, Goldman-Rakic PS. Noise stress impairs prefrontal cortical cognitive function in monkeys: evidence for a hyperdopaminergic mechanism. *Arch Gen Psychiatry*. 1998:55(4):362–368.

Basar-Eroglu C, Brand A, Hildebrandt H, Karolina Kedzior K, Mathes B, Schmiedt C. Working memory related gamma oscillations in schizophrenia patients. *Int J Psychophysiol*. 2007:64(1): 39–45.

Batuev AS, Kursina NP, Shutov AP. Unit activity of the medial wall of the frontal cortex during delayed performance in rats. *Behav Brain Res*. 1990:41(2):95–102.

Becker AB, Warm JS, Dember WN, Hancock PA. Effects of jet engine noise and performance feedback on perceived workload in a monitoring task. *Int J Aviat Psychol*. 1995:5(1):49–62.

Berke JD, Okatan M, Skurski J, Eichenbaum HB. Oscillatory entrainment of striatal neurons in freely moving rats. *Neuron*. 2004:43(6): 883–896.

Berridge CW, Waterhouse BD. The locus coeruleus-noradrenergic system: modulation of behavioral state and state-dependent cognitive processes. *Brain Res Rev*. 2003:42(1):33–84.

Bonnefond M, Jensen O. Alpha oscillations serve to protect working memory maintenance against anticipated distracters. *Curr Biol*. 2012:22(20):1969–1974.

Broadbent DE. *Decision and stress*. London, New York: Academic P; 1971.

Buzsaki G. Theta rhythm of navigation: link between path integration and landmark navigation, episodic and semantic memory. *Hippocampus*. 2005:15(7):827–840.

Buzsaki G. Neural syntax: cell assemblies, synapsembles, and readers. *Neuron*. 2010:68(3):362–385.

Cervera-Ferri A, Guerrero-Martinez J, Bataller-Mompean M, Taberner-Cortes A, Martinez-Ricos J, Ruiz-Torner A, Teruel-Marti V. Theta synchronization between the hippocampus and the nucleus incertus in urethane-anesthetized rats. *Exp Brain Res*. 2011:211(2):177–192.

Cohen MX. *Analyzing neural time series data: theory and practice*. Cambridge (MA): The MIT Press; 2014

Davis M, Whalen PJ. The amygdala: vigilance and emotion. *Mol Psychiatry*. 2001:6(1):13–34.

DeCoteau WE, Thorn C, Gibson DJ, Courtemanche R, Mitra P, Kubota Y, Graybiel AM. Learning-related coordination of striatal and hippocampal theta rhythms during acquisition of a procedural maze task. *Proc Natl Acad Sci U S A*. 2007:104(13): 5644–5649.

Devilbiss DM, Jenison RL, Berridge CW. Stress-induced impairment of a working memory task: role of spiking rate and spiking history predicted discharge. *PLoS Comput Biol*. 2012:8(9):e1002681.

Devilbiss DM, Spencer RC, Berridge CW. Stress degrades prefrontal cortex neuronal coding of goal-directed behavior. *Cereb Cortex*. 2017:27(5):2970–2983.

Dunn AJ. Stress-related changes in cerebral catecholamine and indoleamine metabolism: lack of effect of adrenalectomy and corticosterone. *J Neurochem*. 1988:51(2):406–412.

Freunberger R, Werkle-Bergner M, Griesmayr B, Lindenberger U, Klimesch W. Brain oscillatory correlates of working memory constraints. *Brain Res*. 2011:1375:93–102.

Friedman A, Homma D, Bloem B, Gibb LG, Amemori KI, Hu D, Delcasso S, Truong TF, Yang J, Hood AS, et al. Chronic stress alters striosome-circuit dynamics, leading to aberrant decision-making. *Cell*. 2017:171(5):1191–1205.e28.

Fuster JM, Alexander GE. Neuron activity related to short-term memory. *Science*. 1971:173(3997):652–654.

Gartner M, Rohde-Liebenau L, Grimm S, Bajbouj M. Working memory-related frontal theta activity is decreased under acute stress. *Psychoneuroendocrinology*. 2014:43:105–113.

Gevins A, Smith ME, McEvoy L, Yu D. High-resolution EEG mapping of cortical activation related to working memory: effects of task difficulty, type of processing, and practice. *Cereb Cortex*. 1997:7(4): 374–385.

Ghosal S, Duman CH, Liu RJ, Wu M, Terwilliger R, Girgenti MJ, Wohleb E, Fogaca MV, Teichman EM, Hare B, et al. Ketamine rapidly reverses stress-induced impairments in GABAergic transmission in the prefrontal cortex in male rodents. *Neurobiol Dis*. 2020:134:104669.

Goldman PS, Rosvold HE. The effects of selective caudate lesions in infant and juvenile rhesus monkeys. *Brain Res*. 1972:43(1):53–66.

Goldman-Rakic PS. Cellular basis of working memory. *Neuron*. 1995:14(3):477–485.

Goldman-Rakic PS. The prefrontal landscape: implications of functional architecture for understanding human mentation and the central executive. *Philos Trans R Soc Lond Ser B Biol Sci*. 1996:351(1346):1445–1453.

Hartley LR, Adams RG. Effect of noise on the Stroop test. *J Exp Psychol*. 1974:102(1):62–66.

Heilbronner SR, Rodriguez-Romaguera J, Quirk GJ, Groenewegen HJ, Haber SN. Circuit-based corticostriatal homologies between rat and primate. *Biol Psychiatry*. 2016:80(7):509–521.

Hilton MF, Whiteford HA. Associations between psychological distress, workplace accidents, workplace failures and workplace successes. *Int Arch Occup Environ Health*. 2010:83(8):923–933.

Holmes A, Wellman CL. Stress-induced prefrontal reorganization and executive dysfunction in rodents. *Neurosci Biobehav Rev*. 2009:33(6):773–783.

Horst NK, Laubach M. The role of rat dorsomedial prefrontal cortex in spatial working memory. *Neuroscience*. 2009:164(2):444–456.

Hsieh LT, Ranganath C. Frontal midline theta oscillations during working memory maintenance and episodic encoding and retrieval. *NeuroImage*. 2014:85(0 2):721–729.

Hupalo S, Martin AJ, Green RK, Devilbiss DM, Berridge CW. Prefrontal Corticotropin-releasing factor (CRF) neurons act locally to modulate frontostriatal cognition and circuit function. *J Neurosci*. 2019:39(11):2080–2090.

Jensen O, Tesche CD. Frontal theta activity in humans increases with memory load in a working memory task. *Eur J Neurosci*. 2002:15(8): 1395–1399.

Klimesch W. EEG alpha and theta oscillations reflect cognitive and memory performance: a review and analysis. *Brain Res Rev*. 1999:29(2–3):169–195.

Kramis R, Vanderwolf CH, Bland BH. Two types of hippocampal rhythmical slow activity in both the rabbit and the rat: relations

to behavior and effects of atropine, diethyl ether, urethane, and pentobarbital. *Exp Neurol*. 1975:49(1):58–85.

Levy R, Friedman HR, Davachi L, Goldman-Rakic PS. Differential activation of the caudate nucleus in primates performing spatial and nonspatial working memory tasks. *J Neurosci*. 1997:17(10): 3870–3882.

Manza P, Zhang S, Hu S, Chao HH, Leung HC, Li CR. The effects of age on resting state functional connectivity of the basal ganglia from young to middle adulthood. *NeuroImage*. 2015:107:311–322.

McKlveen JM, Morano RL, Fitzgerald M, Zoubovsky S, Cassella SN, Scheimann JR, Ghosal S, Mahbod P, Packard BA, Myers B, et al. Chronic stress increases prefrontal inhibition: a mechanism for stress-induced prefrontal dysfunction. *Biol Psychiatry*. 2016:80(10): 754–764.

Miller EK, Cohen JD. An integrative theory of prefrontal cortex function. *Ann Rev Neurosci*. 2001:24(1):167–202.

Minguillon J, Lopez-Gordo MA, Pelayo F. Stress assessment by prefrontal relative gamma. *Front Comput Neurosci*. 2016:10:101.

Mitchell DJ, McNaughton N, Flanagan D, Kirk IJ. Frontal-midline theta from the perspective of hippocampal "theta". *Prog Neurobiol*. 2008:86(3):156–185.

Mitchell JF, Sundberg KA, Reynolds JH. Differential attention-dependent response modulation across cell classes in macaque visual area V4. *Neuron*. 2007:55(1):131–141.

Moon SY, Choi YB, Jung HK, Lee YI, Choi SH. Increased frontal gamma and posterior delta powers as potential neurophysiological correlates differentiating posttraumatic stress disorder from anxiety disorders. *Psychiatry Investig*. 2018:15(11):1087–1093.

Mouchati PR, Kloc ML, Holmes GL, White SL, Barry JM. Optogenetic "low-theta" pacing of the septohippocampal circuit is sufficient for spatial goal finding and is influenced by behavioral state and cognitive demand. *Hippocampus*. 2020:30(11):1167–1193.

Oppenheim AV, Schafer RW. *Discrete-time signal processing*. Englewood Cliffs: Prentice-Hall, Inc.; 1989.

Page CE, Coutellier L. Prefrontal excitatory/inhibitory balance in stress and emotional disorders: evidence for over-inhibition. *Neurosci Biobehav Rev*. 2019:105:39–51.

Popescu M, Hughes JD, Popescu EA, Riedy G, DeGraba TJ. Reduced prefrontal MEG alpha-band power in mild traumatic brain injury with associated posttraumatic stress disorder symptoms. *Clin Neurophysiol*. 2016:127(9):3075–3085.

Popescu M, Popescu EA, DeGraba TJ, Fernandez-Fidalgo DJ, Riedy G, Hughes JD. Post-traumatic stress disorder is associated with altered modulation of prefrontal alpha band oscillations during working memory. *Clin Neurophysiol*. 2019:130(10):1869–1881.

Ragozzino ME. The contribution of the medial prefrontal cortex, orbitofrontal cortex, and dorsomedial striatum to behavioral flexibility. *Ann N Y Acad Sci*. 2007:1121(1): 355–375.

Rebec GV, White IM, Puotz JK. Responses of neurons in dorsal striatum during amphetamine-induced focused stereotypy. *Psychopharmacology*. 1997:130(4):343–351.

Roux F, Uhlhaas PJ. Working memory and neural oscillations: alpha-gamma versus theta-gamma codes for distinct WM information? *Trends Cogn Sci*. 2014:18(1):16–25.

Schultz W, Romo R. Neuronal activity in the monkey striatum during the initiation of movements. *Exp Brain Res*. 1988:71(2):431–436.

Spencer RC, Berridge CW. Receptor and circuit mechanisms underlying differential procognitive actions of psychostimulants. *Neuropsychopharmacology*. 2019:44(10):1820–1827.

Spencer RC, Klein RM, Berridge CW. Psychostimulants act within the prefrontal cortex to improve cognitive function. *Biol Psychiatry*. 2012:72(3):221–227.

Strelets VB, Garakh ZV, Novototskii-Vlasov VY. Comparative study of the gamma rhythm in normal conditions, during examination stress, and in patients with first depressive episode. *Neurosci Behav Physiol*. 2007:37(4):387–394.

Surmeier DJ, Ding J, Day M, Wang Z, Shen W. D1 and D2 dopamine-receptor modulation of striatal glutamatergic signaling in striatal medium spiny neurons. *Trends Neurosci*. 2007:30(5): 228–235.

Szalma JL, Hancock PA. Noise effects on human performance: a meta-analytic synthesis. *Psychol Bull*. 2011:137(4):682–707.

Thierry AM, Tassin JP, Blanc G, Glowinski J. Selective activation of mesocortical DA system by stress. *Nature*. 1976:263(5574): 242–244.

Tort AB, Fontanini A, Kramer MA, Jones-Lush LM, Kopell NJ, Katz DB. Cortical networks produce three distinct 7-12 Hz rhythms during single sensory responses in the awake rat. *J Neurosci*. 2010:30(12): 4315–4324.

Vanderwolf CH, Robinson TE. Reticulo-cortical activity and behavior: a critique of the arousal theory and a new synthesis. *Behav Brain Sci*. 1981:4(3):459–476.

van der Meer MA, Redish AD. Low and high gamma oscillations in rat ventral striatum have distinct relationships to behavior, reward, and spiking activity on a learned spatial decision task. *Front Integr Neurosci*. 2009:3:9.

Voorn P, Vanderschuren LJ, Groenewegen HJ, Robbins TW, Pennartz CM. Putting a spin on the dorsal-ventral divide of the striatum. *Trends Neurosci*. 2004:27(8):468–474.